Langmuir
Article
pubs.acs.org/Langmuir

Effects of PEO−PPO−PEO Triblock Copolymers on Phospholipid Membrane Integrity under Osmotic Stress

Jia-Yu Wang,[†] Jaemin Chin,[†] Jeremy D. Marks,[‡] and Ka Yee C. Lee*,[†]

[†]*Department of Chemistry, the Institute for Biophysical Dynamics & the James Franck Institute and* [‡]*Department of Pediatrics, University of Chicago, Chicago, Illinois 60637*

Received May 7, 2010. Revised Manuscript Received June 21, 2010

The effects of PEO−PPO−PEO triblock copolymers, mainly Poloxamer 188, on phospholipid membrane integrity under osmotic gradients were explored using giant unilamellar vesicles (GUVs). Fluorescence leakage assays showed two opposing effects of P188 on the structural integrity of GUVs depending on the duration of their incubation time. A two-state transition mechanism of interaction between the triblock copolymers and the phospholipid membrane is proposed: an adsorption (I) and an insertion (II) state. While the triblock copolymer in state I acts to moderately retard the leakage, their insertion in state II perturbs the lipid packing, thus increasing the membrane permeability. Our results suggest that the biomedical application of PEO−PPO−PEO triblock copolymers, either as cell membrane resealing agents or as accelerators for drug delivery, is directed by the delicate balance between these two states.

Introduction

The cell membrane is in essence an integral lipid bilayer decorated by proteins and carbohydrates. It separates the interior of a cell from the exterior environment and serves as a permeable barrier and controls the passage of large molecules and ions into and out of the cell. The integrity of the cell membrane can be easily compromised by a variety of stimuli, such as thermal burns, barometric trauma, radiation injury, frostbite, and electrical shock. These conditions can cause the cell membrane to lose its barrier function, which may eventually induce cell death.[1] Under normal circumstances, puncturing the cell membrane invokes a rapid resealing response of the cell,[2] which is highly dependent on lipid production and exocytotic lipid delivery to the plasma membrane. This self-sealing mechanism, however, can be substantially slowed or blocked by severe damage induced by various types of injury. In fact, cell membrane dysfunction due to loss of structure integrity is a central pathophysiologic event in many illnesses, including high-voltage electrical trauma[3] and acute neurodegeneration.[4]

Poloxamer 188 (P188, also known as Pluronic F68, $M_w \sim 8400$ Da), a member of a family of surface-active triblock copolymers known as poloxamers[5] consisting of a hydrophobic poly(propylene oxide) (PPO) block joined by identical hydrophilic poly(ethylene oxide) (PEO) blocks at the two ends, has been shown to greatly accelerate resealing of damaged cell membranes.[6−11] However, the fundamental mechanisms involved in P188-mediated cell membrane resealing remain unclear. Previously, studies employing lipid monolayers, supported bilayers, and liposomes as model systems explore the role of triblock copolymers in membrane resealing.[12−20] Results of these studies, however, can drastically differ, depending on the particular model system used. For example, studies employing Langmuir monolayers[13] and supported bilayers[20] have suggested that the triblock copolymers stabilize damaged lipid membranes through selective insertion into low lipid-density regions of the membrane, corralling lipid molecules to pack tightly. In contrast, studies employing large unilamellar vesicles (LUVs) reveal that insertion of the triblock copolymers into lipid bilayers disturbs lipid packing in the membrane, enhancing membrane permeability.[16−19] It is not difficult to pinpoint the root of the inconsistencies in various model systems as each model only mimics a certain aspect of the structural features of the biological membrane. To resolve these seemingly conflicting results, it requires a model system that is simple and yet close enough to the plasma membrane to investigate the effects of triblock copolymers on the structural integrity of the membrane. Single GUVs with diameters in a 10−50 μm range have been widely used as three-dimensional mimics of the cell membrane for investigation of membrane elasticity,[21] domain formation,[22] membrane fusion,[23] vesicle fission,[24] etc. Because of

*To whom correspondence should be addressed. E-mail: kayeelee@uchicago.edu.

(1) Chang, D. C.; Reese, T. S. *Biophys. J.* **1990**, *58*, 1.
(2) Steinhardt, R. A. *Ann. N.Y. Acad. Sci.* **2005**, *1066*, 152.
(3) Lee, R. C.; Kolodney, M. S. *Plast. Reconstr. Surg.* **1987**, *80*, 672.
(4) Shi, R.; Luo, J.; Peasley, M. *Neoroscience* **2002**, *115*, 337.
(5) Alexandridis, P.; Hatton, T. A. *Colloids Surf., A* **1995**, *96*, 1.
(6) Lee, R. C.; River, L. P.; Pan, F.-S.; Ji, L.; Wollmann, R. L. *Proc. Natl. Acad. Sci. U.S.A.* **1992**, *89*, 4524.
(7) Yasuda, S.; Townsend, D.; Michele, D. E.; Favre, E. G.; Day, S. M.; Metzger, J. M. *Nature* **2005**, *436*, 1025.
(8) Marks, J. D.; Pan, C.-Y.; Bushell, T.; Cromie, W.; Lee, R. C. *FAEBS J.* **2001**, *15*, 1107.
(9) Bansal, D.; Mlyake, K.; Vogel, S. S.; Groh, S.; Chen, C.-C.; Williamson, R.; McNeil, P. L.; Campbell, K. P. *Nature* **2003**, *423*, 168.
(10) Serbest, G.; Horwitz, J.; Barbee, K. *J. Neurotrauma* **2005**, *22*, 119.
(11) Ng, R.; Metzger, J. M.; Claflin, D. R.; Faulkner, J. A. *Am. J. Physiol. Cell Physiol.* **2008**, *295*, 146.
(12) Maskarinec, S. A.; Hannig, J.; Lee, R. C.; Lee, K. Y. C. *Biophys. J.* **2002**, *82*, 1453.
(13) Wu, G.; Majewski, J.; Eye, C.; Kjaer, K.; Weygand, M. J.; Lee, K. Y. C. *Phys. Rev. Lett.* **2004**, *93*, 028101.
(14) Frey, S. L.; Lee, K. Y. C. *Langmuir* **2007**, *23*, 2631.
(15) Lee, B.; Firestone, M. A. *Biomacromolecules* **2008**, *9*, 1541.
(16) Johnsson, M.; Bergstrand, N.; Edwards, K.; Stigren, J. R. *Langmuir* **2001**, *17*, 3902.
(17) Demina, T.; Grozdova, I.; Krylova, O.; Zhirnov, A.; Istratov, V.; Frey, H.; Kautz, H.; Melik-Nubarov, N. *Biochemistry* **2005**, *44*, 4042.
(18) Kostarelos, K.; Tadros, Th. F.; Luckham, P. F. *Langmuir* **1999**, *15*, 369.
(19) Krylova, O. O.; Melik-Nubarov, N. S.; Badun, G. A.; Ksenofontov, A. L.; Menger, F. M.; Yaroslavov, A. A. *Chem.—Eur. J.* **2003**, *9*, 3930.
(20) Wu, G.; Majewski, J.; Ege, C.; Kjaer, K.; Weygand, M. J.; Lee, K. Y. C. *Biophys. J.* **2005**, *89*, 3159.
(21) Evans, E.; Rawicz, W. *Phys. Rev. Lett.* **1990**, *64*, 2094.
(22) Veatch, S. L.; Keller, S. L. *Phys. Rev. Lett.* **2002**, *89*, 268101.
(23) Tanaka, T.; Yamazaki, M. *Langmuir* **2004**, *20*, 5160.
(24) Tanaka, T.; Sano, R.; Yamashita, Y.; Yamashita, M. *Langmuir* **2004**, *20*, 9526.

the large size and the ease of observation with optical microscopy, experiments using the single GUV method have revealed more detailed information (such as changes in size and shape) than those using LUVs. For instance, experiments from single GUV leakage by Tamba et al.[25] indicate that the formation of pores due to peptide/lipid interactions, rather than the rate at which materials escape through the pore as proposed from LUV results, is the rate-determining step for the leakage process.

In this work, we directly monitored the loss of structural integrity of single fluorescent dye-loaded GUVs and the effects of triblock copolymers on these damaged membranes using time-lapse fluorescence microscopy. Loss of structural integrity due to decreasing GUV lipid packing density was induced by the application of hypo-osmotic stress, which caused GUVs to undergo substantial structural modifications similar to those exhibited by cells after trauma.[26] The triblock copolymer, mainly P188, was introduced into GUVs system either by perfusion or by preincubation. We have observed two opposing effects of P188 on GUV leakage that critically depends on the location of the polymer with respect to the membrane: the insertion of P188 into the lipid bilayer compromises lipid packing and enhances membrane permeability; in contrast, the adsorption of P188 to the membrane moderately extends GUV swelling, retarding the leakage of intra-GUV content. Our results suggest a two-state interaction mechanism between triblock copolymers and the lipid membrane: state I consists of polymer adsorption onto the lipid bilayer; state II involves polymer insertion into the membrane. The triblock copolymer in state I slows down GUV swelling and retards leakage, thus stabilizing membrane structural integrity. However, because of the mismatch in size and hydrophobicity between the PPO block and the lipid hydrocarbon tails, insertion of the triblock copolymer in state II disrupts lipid packing, increasing membrane permeability. The balance between adsorption and insertion thus appears to dictate the function of the triblock copolymer: it either accelerates resealing of damaged membrane when adsorbed or enhances membrane permeation when inserted. Our ζ-potential measurements indicate that the triblock copolymers adsorb to the lipid membrane at a similar rate below their critical micellar concentration. In contrast, our leakage assay suggests that polymer insertion into the bilayer occurs to different degrees depending on the poloxamer hydrophobicity. In order to elucidate how the hydrophobic block disrupts lipid packing, we have also examined other polymeric constructs that better match the hydrophobic lipid core or does not have the hydrophobic moiety. Our findings show that the hydrophobicity of the copolymer is one of the key elements in determining the biomedical application of poloxamers, either as cell membrane resealing agents or as accelerators for drug delivery.

Materials and Methods

1-Palmitoyl-2-oleoyl-*sn*-glycero-3-phosphocholine (POPC), 1-palmitoyl-2-oleoyl-*sn*-glycero-3-(phosphor-*rac*-(1-glycerol)) (sodium salt) (POPG), 1,2-dioleoyl-*sn*-glycero-3-phosphoethanolamine-*N*-(cap biotinyl) (sodium salt) (Biotin-PE), and 1,2-dioleoyl-*sn*-glycero-3-phosphoethanolamine-*N*-(methoxy(poly(ethylene glycol))-3000) (ammonium salt) (PEG3000-PE) in chloroform (5 mg/mL) were purchased from Avanti Polar Lipids (Alabaster, AL). Texas Red-1,2-dihexa-decanoyl-*sn*-glycero-3-phosphoethanolamine, triethylammonium salt (TR-DHPE), and Alexa Fluoro 488 hydrazide (sodium salt) were purchased in powder from Molecular Probes, Inc. (Carlsbad, CA). The triblock copolymers P188, P338, P407, and P181 were generous gifts of the BASF Corp., and their detailed molecular structure can be found in Table 1. Three lipid mixtures were used to make GUVs: POPC/POPG/Biotin-PE/TR-DHPE (88/10/1/1 in mol ratio), POPC/POPG/Biotin-PE/TR-DHPE/P188 (87.9/10/1/1/0.1), and POPC/POPG/Biotin-PE/TR-DHPE/PEG-3000-PE (87.8/10/1/1/0.2) and will be referred to as GUV, P188-GUV, and PEG-PE-GUV, respectively, in the rest of the article. The use of biotin-PE was to immobilize the vesicles onto a streptavidin-functionalized glass coverslip through the receptor−ligand pair, streptavidin−biotin.[27] The use of 10% charged lipid POPG was to provide the electrostatic repulsion between GUVs so as to prevent GUVs from aggregation.[28] GUVs were made by the electroformation method.[29] To immobilize GUVs, the suspension of GUVs (~50 μM/mL) was initially injected into the chamber gently and then incubated for ~15−30 min so as to allow for the GUVs to settle and be tethered to the bottom substrate of the flow chamber. The excess untethered GUVs were then flushed by perfusion of an iso-osmotic glucose solution. This process was controlled by a syringe pump (Harvard Apparatus, Holliston, MA) at a flow rate of less than 12 μL/min. The flow in the chamber was tested by a dye solution and could be adequately approximated as laminar flow. To apply hypo-osmotic gradients to GUVs, a flow chamber with an internal volume of less than 70 μL (RC-30; Warner Instruments, Hamden, CT) was used. Details for GUV preparation and flow chamber configuration can be found in the Supporting Information.

Table 1. Summary of the Examined $(PEO)_{m/2}(PPO)_n(PEO)_{m/2}$ Triblock Copolymers[a]

poloxamers	M_w (g/mol)	m	n	PO/EO	HLB	PDI
P188	8400	80	27	2/8	29	1.08
P388	14600	141	44	2/8	27	1.15
P407	12600	101	56	3/7	22	1.22
P181	1750	2	32	9/1	3	1.18

[a] m: the total unit number of EO; n: the total unit number of PO; HLB: hydrophile−lipophile balance, a high HLB value indicates a more hydrophilic polymer while a low HLB value indictates a more lipophilic polymer; PDI: polydispersity index.

The hypo-osmotic stress was applied to GUVs by exchanging the iso-osmotic glucose solution in the flow chamber to a glucose solution of a lower osmolarity at a flow rate of 8 μL/min. The triblock copolymers were introduced into the flow chamber by perfusing a polymer/glucose solution of the desired osmolarity. The hypo-osmotic gradient, $\Delta\pi$, was estimated as $\Delta\pi = C_{in} - C_{out}$, where C_{in} is the osmolarity of the sucrose solution inside of GUVs and C_{out} is that of the glucose solution perfused into the chamber. All experiments were performed at room temperature. For each experiment, there were more than 30 GUVs tethered to the substrate; a single isolated GUV of size 35−45 μm was monitored by time-lapse fluorescence microscopy, and its response to the hypo-osmotic stress was compared with the rest of the GUVs in the chamber at the end of the experiment. Since GUVs formed by the electroformation method can have highly heterogeneous initial membrane tension, they show different responses to the applied osmotic stress. For GUVs with extremely high membrane tension, they are very unstable and rupture upon sedimentation to the bottom substrate after initial injection to the sample chamber (~20% of total GUVs in a given experiment); for GUVs with high membrane tension, they either completely leak out or rupture at the examined stress (~30% of total GUVs). In this work, only results from the stable GUVs, that is, GUVs with relatively low membrane tensions, which were estimated to be less than 4.2 ± 1.9 mN/m (detailed derivation can be found in ref 30)

(25) Tamba, Y.; Ohba, S.; Kubota, M.; Yoshioka, H.; Yoshilka, H. *Biophys. J.* **2007**, *92*, 3178.
(26) Marks, J. D.; Bindokas, V. P.; Zhang, X. M. *Brain Res. Dev. Brain Res.* **2000**, *124*, 101.
(27) Stamou, D.; Duschl, C.; Delamarche, E.; Vogel, H. *Angew. Chem., Int. Ed.* **2003**, *42*, 5580.
(28) Lipowsky, R. *Nature* **1991**, *349*, 475.
(29) Angelova, M. I.; Soleau, S.; Meleard, P.; Faucon, J.; Bothorel, P. *Prog. Colloid Polym. Sci.* **1992**, *89*, 127.

were taken into account. Data reported here are from experiments where over 50% of total GUVs in the same set (i.e., approximately all of the GUVs with relatively low membrane tensions) showed a similar behavior. A distribution of GUV response to a hypo-osmotic gradient of 40 mOsm is included in the Supporting Information to provide a representative illustration of the statistic in a given experiment; experiments were performed in triplicates to check for reproducibility.

The confocal image stacks for 3D reconstruction of the tethered GUV were acquired on a laser scanning confocal microscope (Leica TCS SP2 AOBS) in the Integrated Microscopy Core Facility at the University of Chicago. Fluorescence micrographs in the leakage assay were acquired on a vertical optical microscope (Nikon ME600) with a cooled CCD camera (Hamamatsu ORCA-ER) connected to a PC running the Simple PCI software (Compix Inc., Sewichley, PA). The microscope was motorized so that fluorescence from dye molecules both in the membrane (red) and the solution inside GUVs (green) could be monitored concurrently (with 100 ms retardation during filter switch). The fluorescence intensity profile was obtained by integrating the intensity in regions of interest, which were defined as an area slightly larger than that occupied by the tethered GUV. All time-lapse fluorescence images were background subtracted using the corresponding blank areas as reference. Because of the ease of photobleaching of Texas Red-DHPE in the membrane, the projection diameter of GUVs was analyzed using ImageJ software (NIH, 1.42°) from fluorescence images of the dye Alexa 488 inside of GUVs (green channel). To define the projection contour of GUVs, all images in the same file were confined by the same threshold value. The osmolarity of the sugar solutions was measured by an osmometer, OSMETTE II (Precision System Inc., Natick, MA). The average ζ-potential measurements of GUVs were performed using a Nano-ZS instrument (model ZEN3600, Malvern Instruments, U.K.), and the principle of ζ-potential measurements and the experimental details can be found in the Supporting Information. To avoid GUV sedimentation, ζ-potential measurements were performed in the same sucrose buffer as the hydration solution. As the polymer concentration used in our experiments was very low, zeta potential measurements of such polymer samples in the absence of GUVs yielded no observable results. The ζ-potential measurements reported here are therefore due to the GUVs present in the sample and reflect changes in the GUV signals with polymers present. A discussion on error calculations for our ζ-potential measurements can also be found in the Supporting Information.

Results

Response of GUVs under Hypo-osmotic Gradients. Theoretical calculation[33] and experimental observations[34,35] using large unilamellar vesicle (LUV, 100 nm $< d <$ 500 nm) suspension indicate that LUVs, when subjected to hypo-osmotic gradients, undergo a series of substantial structural modifications. Initially, they swell as an elastic response in an attempt to balance the applied hypo-osmotic gradient. Once a critical gradient is reached, the membrane yields and transient pore formation results in rapid leakage of the interior solution. After the efflux of a sufficient amount of interior solution, vesicles reseal into a mechanically stable structure. Because of the small size of LUVs, this process of structural changes in a single vesicle has never been directly observed. Here, we provide the first direct visualization of the response of a single GUV to hypo-osmotic gradients.

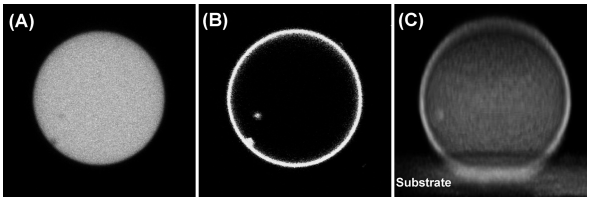

Figure 1. Representative confocal fluorescence images of a tethered GUV: (A) from dye Alexa 488 inside GUV, (B) from dye TR-DHPE in the membrane, and (C) 3D reconstruction of a tethered GUV from dye TR-DHPE in the membrane. Vesicle size: 36 μm.

Figure 1 shows a typical tethered GUV after iso-osmotic flow. Because of the existing membrane tension, GUVs are kept in a spherical shape, with a slight deformation at the location in contact with the substrate. As GUVs remain in this slightly truncated spherical shape throughout the course of the experiment, we have monitored the change in size of the GUV using its projection diameter. A typical time-dependent leakage of Alexa 488 from a single GUV under an iso-osmotic gradient is shown in Figure 2A. Over 30 min, the relative fluorescence intensity, I/I_0, where I_0 is the fluorescence intensity at $t = 0$, only slightly decreased from 1 to 0.986 ± 0.003. Meanwhile, no change in GUV relative diameter, D/D_0 (D_0 is GUV diameter at $t = 0$), was observed (Figure 2F). The small changes in I/I_0 and D/D_0 suggest that under our experimental conditions factors like gravity, surface adhesion, and shear stress from the continuous flow have no effect on the tethered GUVs. Thus, we attribute the decrease in I/I_0 under iso-osmotic conditions to photobleaching of Alexa 488. It should be noted that the chamber was connected to the injection syringe by a short polyethylene tube, and time $t = 0$ was set at the point when the perfusion of hypo-osmotic solution was started. Thus, the length of the polyethylene tube and the distance of the tethered GUV under study from the chamber inlet determined the latency from the initiation of the hypo-osmotic flow to the time that the gradient hit the monitored vesicle. During this latency, I/I_0 and D/D_0 did not change, similar to those observed for an iso-osmotic gradient.

With the onset of a hypo-osmotic front, GUVs began to exhibit structural changes, as determined from observed changes in I/I_0 and D/D_0. Figure 2B−E shows the characteristic time-lapse profiles of I/I_0 at hypo-osmotic gradients, $\Delta\pi$, of 22 ± 3, 45 ± 5, 76 ± 4, and 97 ± 2 mOsm; the corresponding changes in D/D_0 are shown in Figure 2G−J. At $\Delta\pi = 22 \pm 3$ mOsm, a small but consistent decrease in I/I_0 was observed until I/I_0 reached 0.973 ± 0.003, beyond which the intensity remained constant. Meanwhile, D/D_0 started to increase, indicating the swelling of GUVs. This membrane expansion lasted for 246 ± 54 s and then equilibrated at a final diameter of $1.5 \pm 0.6\%$ greater than the initial one. According to ref 33, the swelling mainly involves the influx of water and practically no leakage of the osmotically active substances (Alexa 488 and sucrose in our case); the slight decrease in I/I_0 is likely from the change in the concentration of Alexa 488 due to the expansion. Assuming a spherical geometry for our GUVs and using the relationship between fluorescence intensity and vesicle diameter, $I/I_0 \propto (D_0/D)^2$,[36] an increase of $\sim 1.5 \pm 0.6\%$ in

(30) Since our GUVs are tense, the relative area change $\Delta A/A_0 \sim (D^2 - D_0^2)/D_0^2$. On the basis of the work of micropipet aspiration,[31,32] we use the values of the compressibility moduli, K, and the lysis tension, τ^*, for SOPC, ~192 and 10 mN/m, respectively, for our calculations, since SOPC is structurally very similar to POPC, which is the major lipid component of our GUVs. Assuming $\tau^* = \tau_{applied} + \tau_{membrane} = K\Delta A/A_0 + \tau_{membrane}$, the GUVs in our experiments are found to have an initial membrane tension, $\tau_{membrane}$, of $\sim 4.2 \pm 1.9$ mN/m ($\Delta A/A_0 = 0.03 \pm 0.01$). It should be noted that since we have 10% charged lipid POPG in our GUVs as well, K for our GUVs may be 5−10% higher than that of pure POPC. Taking this into account, the actual initial membrane tension of our GUVs may be even lower than 4.2 mN/m.

(31) Olbrich, K.; Rawicz, W.; Needham, D.; Evans, E. *Biophys. J.* **2000**, *79*, 321.
(32) Simon, S. A.; Mclntosh, T. J.; Magid, A. D.; Needham, D. *Biophys. J.* **1992**, *61*, 786.
(33) Koslov, M. M.; Markin, V. S. *J. Theor. Biol.* **1984**, *109*, 17.
(34) Shoemaker, S. D.; Vanderlick, T. K. *Ind. Eng. Chem. Res.* **2002**, *41*, 324.
(35) Pencer, J.; White, G. F.; Hallett, F. R. *Biophys. J.* **2001**, *81*, 2716.

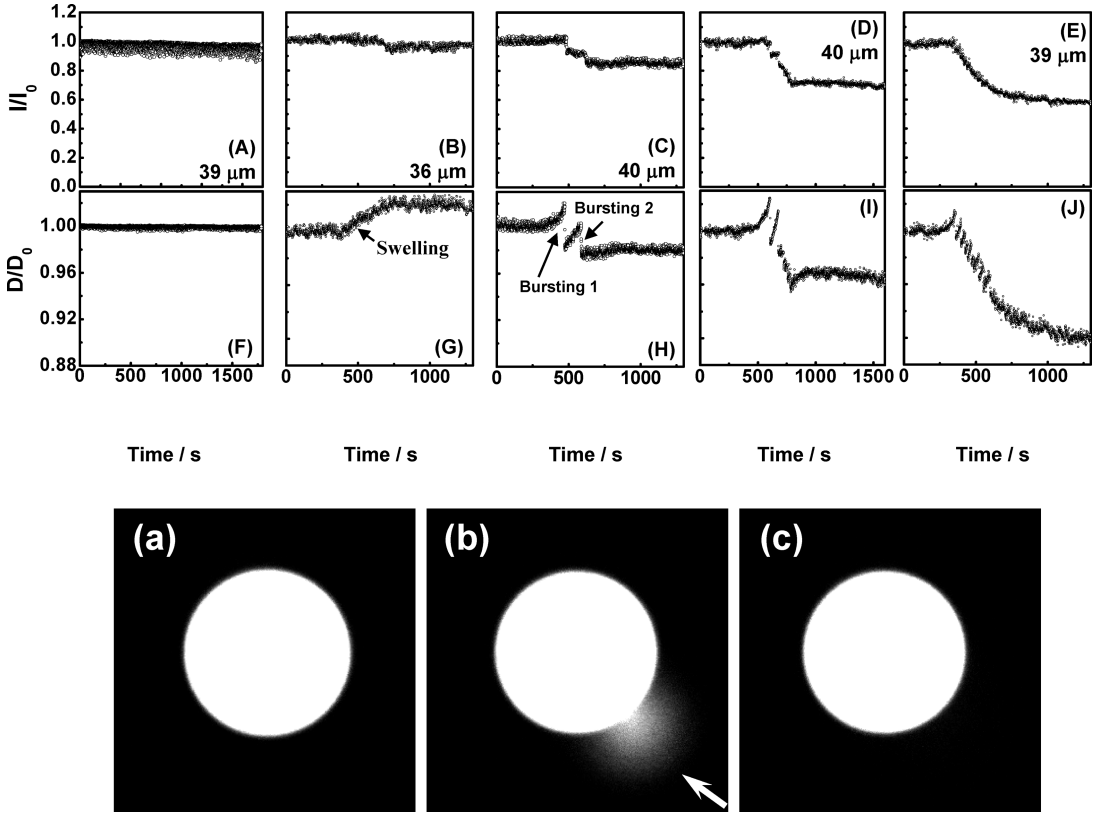

Figure 2. Upper: (A−E) Leakage of Alexa 488 from inside the GUV, measured as a decrease in the relative fluorescence intensity, I/I_0, and (F−J) change in GUV relative diameter, D/D_0, at $\Delta\pi$ = (A, F) 0, (B, G) 22 ± 3, (C, H) 45 ± 5, (D, I) 76 ± 4, and (E, J) 97 ± 2 mOsm as a function of time. The diameters of the examined GUVs are listed. Lower: Fluorescence images of a typical bursting event: (a) the intact vesicle right before bursting; (b) the bursting vesicle, with the ejection of Alexa 488 visible as a bright cloud (indicated by the arrow); (c) the resealed vesicle right after bursting. Frame rate: 0.4 fps; the vesicle size: 39 μm.

diameter should cause a roughly 3 ± 1.2% decrease in I/I_0, which is in good agreement with our observation (3 ± 0.3% decrease). In addition, the change in applied osmolarity difference, C_{out}/C_{in} = 0.933, is close to that in vesicle volume, $V_0/V = (D_0/D)^3 = 0.956$ (see Supporting Information for detailed derivations). These results suggest that the examined GUVs can balance the hypo-osmotic gradient of 20 mOsm by purely elastic swelling.

At $\Delta\pi = 45 \pm 5$ mOsm, pure swelling of GUVs was not enough to balance the osmotic gradient, and bursting events, accompanied by rapid leakage through a giant transient pore which has been observed by several groups,[37−39] occurred. These leakages are better presented in the time-lapse profile of I/I_0 and D/D_0, as shown in Figure 2C,H. For all three independent measurements, the first swelling of the GUVs lasted for 157 ± 73 s before bursting occurred. The first burst usually was not enough to fully release the stress so that the residual osmotic stress continued to cause GUV to swell and then to burst again until the residual stress across the GUV membrane vanished. Images capturing a typical bursting event are shown in Figure 2a−c. At $\Delta\pi \approx 40$ mOsm, I/I_0 eventually decreased to 0.833 ± 0.014 after the final bursting event, and the vesicles remained stable over the rest of the experiment. It should be noted that the bursts did not simply result in the ejection of the interior solution but also involved the loss of phospholipids from the membrane where the bursting event occurred, as evidenced by an average shrinkage of 1.67 ± 0.14% in the GUV diameter and the fluorescence images shown in Supporting Information S-Figure 2. This loss of phospholipids is in good agreement with the third mechanism of lipid loss from the membrane discussed in Portet's work.[40]

GUVs responded in a similar way by exhibiting a series of swelling−bursting cycles when subjected to even higher $\Delta\pi$ between 40 and 100 mOsm. We observed much shorter swelling duration for higher hypo-osmotic gradients, in good agreement with the theoretical prediction that pores form more quickly at higher osmotic gradients.[33] In addition, more of the interior solution was ejected and more phospholipids from the membrane were lost as the hypo-osmotic gradients progressed to higher values (see Table 2 for quantitative comparison). In all three cases of higher hypo-osmotic gradients, the final change in vesicle volume corresponds well with the applied osmolarity difference: at $\Delta\pi = 45 \pm 5$ mOsm, $C_{out}/C_{in} \sim 0.867$, $(D_0/D)^3(I/I_0) \sim 0.899$; at $\Delta\pi = 76 \pm 4$ mOsm, $C_{out}/C_{in} \sim 0.733$, $(D_0/D)^3(I/I_0) \sim 0.732$; at $\Delta\pi = 97 \pm 2$ mOsm, $C_{out}/C_{in} \sim 0.667$, $(D_0/D)^3(I/I_0) \sim 0.713$ (see Supporting Information for detailed derivations). Since no complete disruption or dissolution of the membrane structure was observed for this selected portion of GUVs in the 0−100 mOsm osmotic gradient range examined, we chose to perform the following P188 experiments at $\Delta\pi \leq 100$ mOsm, mainly at ~20 and ~40 mOsm,

(36) The fluorescence intensity, I, is proportional to Φ, where Φ is the quantum yield, and the number of photons adsorbed. According to Beer−Lambert law, the absorbance is linear with the concentration, C, and the path lengh, L. Accordingly, we can get $I \propto CL$. For the single GUV, C is equal to $6m/\pi D^3$, where m is the mass and D is GUV diamter, and L is equal to D. Since there is no loss of dye during swelling, we can derive $I/I_0 \sim D_0^2/D^2$.

(37) Sandre, O.; Moreaux, L.; Brochard-Wyart, F. *Proc. Natl. Acad. Sci. U.S.A.* **1999**, *96*, 10591.

(38) Peterlin, P.; Arrigler, V. *Colloids Surf., B* **2008**, *64*, 77.

(39) Peterlin, P.; Jaklic, G.; Pisanski, T. *Meas. Sci. Technol.* **2009**, *20*, 055801.

(40) Portet, T.; Febrer, F. C.; Escoffre, J.-M.; Favard, C.; Rols, M.-P.; Dean, D. S. *Biophys. J.* **2009**, *96*, 4109.

Table 2. Comparison of GUVs' Response between the Absence and the Perfusion of P188 under Different Hypo-osmotic Gradients

	I/I_0		D/D_0		τ^a	
hypo-osmotic gradient, $\Delta\pi$ (mOsm)	GUV	perfusion of P188	GUV	perfusion of P188	GUV	perfusion of P188
~20	0.973 ± 0.003	0.967 ± 0.002	1.015 ± 0.006	1.013 ± 0.003	$> 246 \pm 54$	$> 236 \pm 31$
~40	0.833 ± 0.014	0.835 ± 0.010	0.975 ± 0.005	0.984 ± 0.005	157 ± 73	101 ± 16
~80	0.660 ± 0.030	0.734 ± 0.009	0.966 ± 0.005	0.972 ± 0.002	104 ± 34	156 ± 47
~100	0.564 ± 0.014	0.616 ± 0.027	0.925 ± 0.003	0.931 ± 0.004	89 ± 27	121 ± 12

[a] τ: duration time of the first swelling.

to investigate the effect of P188 on the structural integrity of GUVs.

Effect of Poloxamer 188 on the Response of GUVs under Hypo-osmotic Gradients. To test the effect of P188 on the compromised membranes, we introduced P188 into the GUV system by continuous perfusion of a hypo-osmotic solution containing 50 μM P188. With this experimental protocol, GUVs are subjected to the action of P188 and the desired hypo-osmotic gradient simultaneously. The overall behavior of GUVs when P188 was introduced by perfusion was, however, rather similar to that when P188 was absent under the same hypo-osmotic gradients: vesicles only swelled at $\Delta\pi \leq 20$ mOsm but started to leak through numerous swelling−bursting cycles at $\Delta\pi > 20$ mOsm (typical time-lapse profiles of I/I_0 and D/D_0 are shown in Supporting Information S-Figure 1). While quantitative comparison between the two cases, with and without P188, as shown in Table 1 suggests subtle differences in the first swelling duration, the loss of the interior solution, and phospholipids from the membrane at high osmotic gradients, these effects, are nevertheless much weaker than what one would expect for a substance which has been demonstrated to be an effective membrane sealant.[6,7]

A natural question then is whether there is enough P188 accumulated at GUV/aqueous solution interface during perfusion to participate in the resealing process. To study the dynamics of P188 accumulation at the membrane surface, we carried out ζ-potential measurements on the GUVs/polymer system as a function of incubation time. It is well-known that ζ-potential measurement is a powerful technique to investigate polymer/lipid membrane adsorption.[41,42] Even though most of the reported work employed LUVs as a model system, the work by Portet et al.[40] and Carvalho et al.[41] indicate that the measurement can also be extended to GUV systems. As shown in Figure 3A, the ζ-potential of the bare GUVs without P188 present is -62.5 ± 10.2 mV. After 3 h of incubation, the ζ-potential of the GUVs/P188 increased to -48.7 ± 8.2 mV and eventually reached its plateau after 2 days of incubation. This result indicates that the dynamics of interaction between P188 and GUVs is indeed slow. The slow dynamics of the interaction between GUVs and P188 in comparison to that of membrane swelling suggests that when the perfusion protocol is used, only a trace amount of P188 can possibly get close to the vesicle/aqueous solution interface before bursting events commence; this small amount of P188 is far from enough to significantly modify the swelling process.

To increase the level of P188 at the membrane surface, GUVs were incubated with 50 μM P188 for 3 h. It should be noted that the applied hypo-osmotic stress was a continuous one, so the only way for the vesicle to balance this stress is through leakage, eventually. Therefore, it is reasonable to expect P188 to retard the leakage but not to eliminate it completely. Indeed, GUVs incubated with P188 swelled over a moderately longer time scale compared to those exposed to P188 by perfusion. For example,

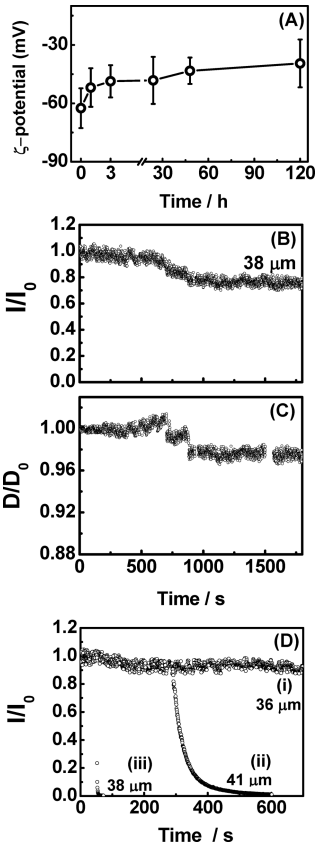

Figure 3. (A) ζ-potential of GUVs in the presence of 50 μM P188 as a function of incubation time. (B) Leakage of Alexa 488, measured as a decrease in the relative fluorescence intensity, I/I_0, and (C) change in relative diameter, D/D_0, of GUV incubated with 50 μM P188 for 3 h at $\Delta\pi = 45 \pm 5$ mOsm as a function of time. The diameter of the examined GUV is 38 μm. (D) Time-lapse leakage of Alexa 488, measured as a decrease in the relative fluorescence intensity, I/I_0, of GUVs incubated with 50 μM P188 for (i) 0, (ii) 1, and (iii) 5 days at $\Delta\pi = 22 \pm 3$ mOsm. The diameters of the examined GUVs are (i) 36, (ii) 41, and (iii) 38 μm.

the first and second swelling of GUVs at $\Delta\pi = 42 \pm 4$ mOsm lasted 343 ± 62 and $176 + 38$ s, respectively, about 2 times longer in duration than those found in the absence of P188, as shown in a typical leakage profile in Figure 3B,C. It has been predicted by Taupin et al.[42] and Koslov et al.[33] that osmotic-stress-induced transient pores result from membrane expansion, and they form only after the membrane expansion exceeds a threshold value. Results from our incubation experiment indicate that P188 has the capability to prolong the swelling duration and thus help retard the leakage.

Since ζ-potential measurements indicate that more P188 reaches the lipid membrane/aqueous solution interface with incubation time, we have further extended the duration of incubation to examine if an even more robust protective effect can be achieved. Surprisingly, a completely opposite effect was

(41) Carvalho, K.; Ramos, L.; Roy, C.; Picart, C. *Biophys. J.* **2008**, *95*, 4348.
(42) Taupin, C.; Dvolaitzky, M.; Sauterey, C. *Biochemistry* **1975**, *14*, 4771.

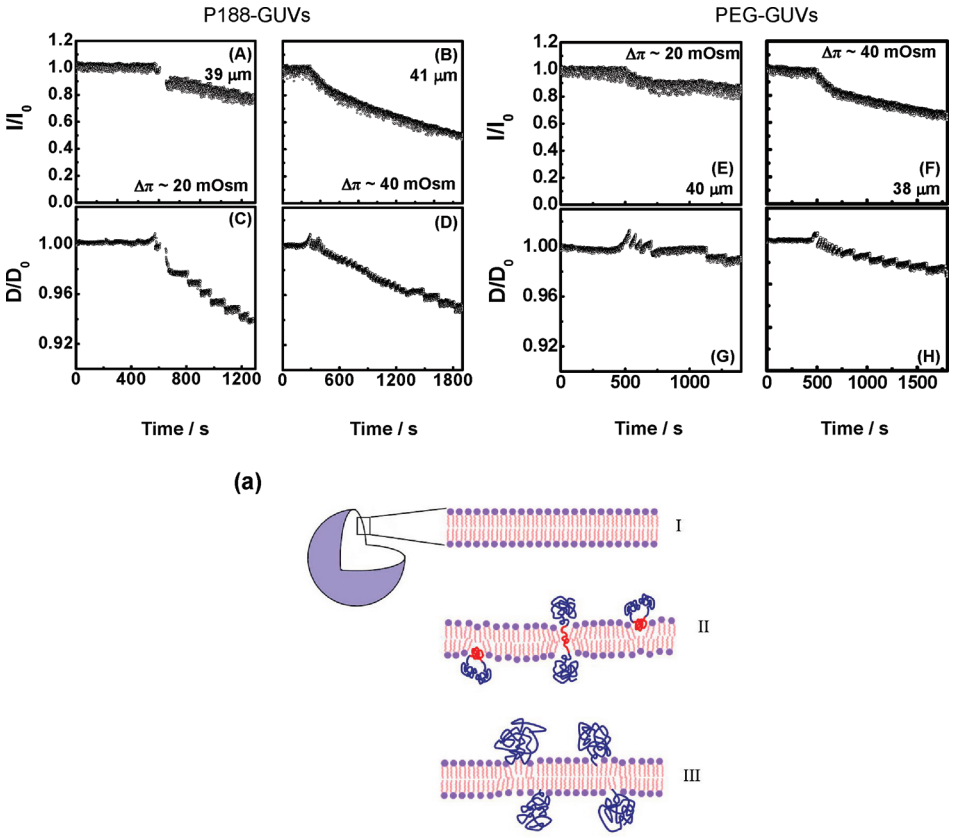

Figure 4. (A−D) P188-GUVs. (E−H) PEG3000-PE-GUVs. (A, B, E, F) Leakage of Alexa 488, measured as a decrease in the relative fluorescence intensity, I/I_0. (C, D, G, H) Change in relative diameter, D/D_0, at $\Delta\pi$ = (A, C, E, G) 22 ± 3, and (B, D, F, H) 45 ± 5 mOsm as a function of time. The diameters of the examined GUVs are listed. (a) Possible lipid packing configurations in (I) GUV, (II) P188-GUV, and (III) PEG-PE-GUV.

observed as all GUVs ruptured after incubating GUVs with P188 for more than 1 day at $\Delta\pi$ = 42 ± 4 mOsm (data not shown). This membrane disruptive effect from a long-time P188 incubation is even more evident at a low gradient. As shown in Figure 3D, GUVs, in the presence of P188 via perfusion, responded to a 24 ± 3 mOsm gradient by pure swelling with no leakage (Figure 3D-i), GUVs incubated with P188 for 1 day, however, released their interior content completely with a characteristic time of ~39 s (Figure 3D-ii) and GUVs incubated with P188 for 5 days ruptured at $\Delta\pi$ = 26 ± 2 mOsm (Figure 3D-iii). This disruptive effect induced by long P188 incubation is reflected not only in the leakage profiles but also in the general stability of the vesicles. In the absence of P188 incubation, GUVs are good for use within a week of their formation, either in their natural sucrose suspension or in a diluted glucose solution. However, with P188 incubation, Alexa 488 trapped in GUVs starts to leak from a small portion of GUVs after 1 day of incubation even under isoosmotic conditions, and the total number of stable GUVs is markedly reduced after 3 days of incubation. (see S-Figure 3). These dramatically different effects of P188 on the structural integrity owing to the difference in the duration of P188 incubation indicate that more than one process might be involved in the interaction of P188 with the lipid membrane.[43]

(43) It should be noted that even though we used a fairly high polymer concentration (lipid to polymer ratio ~ 2.6:1) in the incubation experiments, the amount of P188 incorporated into the membrane after a long period of incubation would be fairly low as P188 did not prefer to incorporate into lipid membranes, which is evidenced by our preincorporation experiments—the yield of GUVs significantly decreased at ratios of lipid to polymer to lower than 99.5:0.5, and no GUVs can be formed at lipid to polymer ratios below 99:1.

Models To Differentiate Various Processes of P188 Interaction with Phospholipid Membranes. We hypothesize that the location of P188 with respect to the membrane plays a key role in terms of their function as either a membrane sealant or a permeation enhancer. To prove this, we designed two models: one has P188 (denoted as P188-GUV), and the other has PEG3000-PE (denoted as PEG-PE-GUV) preincorporated into the lipid membrane. We chose PEG3000-PE because of its similar hydrophilic size compared to P188 but its lack of any mismatch in size or hydrophobicity with the lipid tails. We used the first model to mimic the behavior of GUVs after P188 inserted into the membrane and the second one to mimic the behavior of GUVs that only have P188 adsorbed on the membrane. The incorporation of P188 and PEG3000-PE were confirmed by ζ-potential measurement: ζ increased from −62.5 ± 10.2 mV for the bare GUVs to −48.1 ± 10.7 for P188-GUVs and to −47.8 ± 10.8 mV for PEG-PE-GUVs.

The representative responses of these two types of GUVs at $\Delta\pi$ = 22 ± 2 and 45 ± 5 mOsm are shown in Figure 4. Contrary to the behavior of bare GUVs, P188−GUVs at $\Delta\pi$ = 22 ± 2 mOsm leaked through a series of bursting events, each of which followed by a fairly short and low-degree swelling. Over the measured time, I/I_0 decreased to 0.799 ± 0.03 and D/D_0 dropped to 0.939 ± 0.002 (Figure 4A,C). At $\Delta\pi$ = 45 ± 5 mOsm, I/I_0 further reduced to 0.505 ± 0.013 over the measured time of 2000 s and the dynamics of each swelling−bursting cycle accelerated as well. Interestingly, the profiles of I/I_0 and D/D_0 for the P188−GUVs at a hypoosmotic gradient of 45 ± 5 mOsm (Figure 4B,D) are not similar to those of GUVs incubated with P188 for a short time (Figures 3A) at all but are remarkedly similar to those of GUVs at $\Delta\pi$ = 97 ± 2

mOsm (Figure 2E,J), indicating that the insertion of P188 does not help to restore the structural integrity of the vesicles but disrupts lipid packing and destabilizes GUVs. In fact, this disruption effect was also observed during P188-GUVs formation. We found that the yield of P188-GUVs significantly decreased with increasing P188 concentration in the membrane, and P188-GUVs with more than 0.5 mol % P188 were unstable and easily destroyed by even slight vibrations.

The disruptive effect of P188 insertion into the membrane is most likely due to the mismatch between the PPO block and the hydrocarbon tails of the lipids, in terms of both size and hydrophobicity. To determine if the PPO block is indeed the culprit, PEG-PE-GUVs (0.2 mol %) has been examined. In this case, no mismatch in size or hydrophobicity exists in the lipid tail region, but the presence of the 3 kDa PEG at the membrane surface is secured by anchoring the associated hydrocarbon tail of the large polymer headgroup among hydrocarbon tails of the lipid molecules. Shown in Figure 4E−H are the representative time-lapse profiles of I/I_0 and D/D_0 for PEG-PE-GUVs at $\Delta\pi = 22 \pm 2$ and 45 ± 5 mOsm. In comparison to the profiles of P188-GUVs shown in Figure 4A−D, the leakage and loss of phospholipids from the membrane, under otherwise identical experimental conditions, are reduced for PEG-PE-GUVs, confirming the disruptive effect of the PPO block. However, the disruptive effect is not completely blocked under the experimental conditions examined, and leakage through swelling−bursting cycles even exists at $\Delta\pi = 22 \pm 2$ mOsm, whereas bare GUVs only swelled at this low hypo-osmotic gradient. These results thus indicate that the large headgroup of PEG still has a compromising effect, albeit much reduced compared to that of the PPO block, on lipid packing. A cartoon depicting possible lipid packing configurations in GUV, P188-GUV, and PEG-PE-GUV based on our experimental observations is shown in Figure 4a.

The disruptive effect was found to be completely blocked when PEG, which does not have the hydrophobic acyl chain, was used in place of PEG-PE. This was achieved by the perfusion of high molecular weight PEG (20 kDa) of 1 wt % to the tethered GUVs along with the hypo-osmotic glucose solution. As shown in Figure 5, GUVs, in the presence of PEG at $\Delta\pi = 45 \pm 5$ mOsm, leak less and swell longer than those with P188 and PEG2000-PE incorporation (Figures 4). ζ-potential measurements show an increase in ζ from -62.5 ± 10.2 mV for the bare GUVs to -41.3 ± 9.28 mV for GUVs incubated with 1 wt % of PEG 20 kDa. It is well-known that PEG does not insert into lipid membranes; the increase in ζ-potential therefore indicates the accumulation of PEG near the GUV surface. The driving force to bring PEG close to the lipid membrane surface likely stems from the dehydration effect of PEG.[44] Consequently, the similarity of the extended swelling observed both in the short-time incubation with P188 and perfusion of PEG 20 kDa points to the fact that the modification of the swelling process induced by P188 originates from the physical adsorption of the polymer near the membrane surface but not through the insertion process, as shown in Figure 5a.

Effects of Poloxamer Hydrophobicity on the Mode of Interaction with Lipid Membranes. In order to test how the size of the hydrophobic block and the hydrophobic/hydrophilic ratio of the poloxamer affect its interactions with the membrane, we have carried out both ζ-potential and leakage assays using other poloxamers, P181, P338, and P407 and have compared their behavior to that of P188. The ζ-potential measurements shown in Figure 6A suggest that the triblock copolymers with different

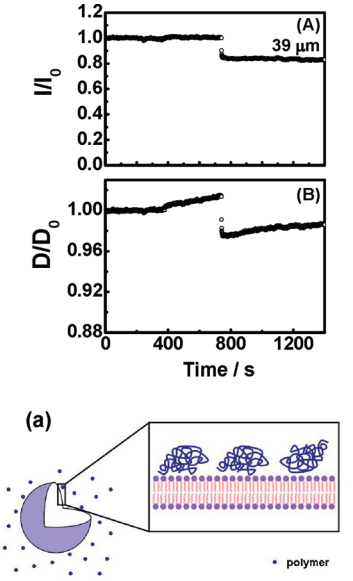

Figure 5. (A) Leakage of Alexa 488, measured as a decrease in the relative fluorescence intensity, I/I_0, and (B) change in relative diameter, D/D_0, of GUV upon perfusion of 1% (wt) PEG 20 kDa at $\Delta\pi = 45 \pm 5$ mOsm as a function of time. The diameters of the examined GUVs are listed. (a) Possible location of P188 and PEG to the membrane surface induced by perfusion and short-time incubation.

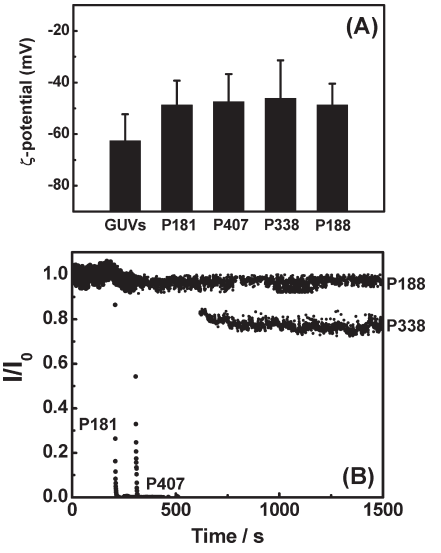

Figure 6. (A) ζ-potential of GUVs and GUVs incubated with P181, P407, P338, and P188 for less than 3 h. (B) Time lapse of leakage of Alexa 488, measured as a decrease in the relative fluorescence intensity, I/I_0, upon perfusion of P188, P338, P407, and P181 at $\Delta\pi = 23 \pm 2$ mOsm.

hydrophobicity have a very similar capability to accumulate on the membrane surface when administered below their CMC values, regardless of the size of the polymer chains. The leakage experiments in Figure 6B, on the other hand, show that the insertion capability of the triblock copolymers correlates well with their hydrophobicity. For instance, at $\Delta\pi \sim 20$ mOsm, the introduction of P181 and P407 by perfusion induces the rupture of GUVs, and P338 causes severe leakage, whereas P188 slightly prolong the swelling. It should be noted that the change in ζ-potential induced by the polymers came from the shielding effect of PEO; ζ-potential measurements are insensitive to the

(44) Lehtonen, J. Y. A.; Kinnumen, P. K. *Biophys. J.* **1995**, *68*, 525.

location of PPO block and cannot differentiate between PPO adsorption vs PPO insertion. The disruptive effect on the stability of the GUVs observed in our leakage experiments, on the other hand, came from the insertion of the PPO block into the lipid membrane. Therefore, results from our leakage experiments provide direct information on the mode of poloxamer interaction, i.e., the capability of poloxamer to insert its PPO block into the lipid membrane, which is mainly dictated by the overall hydrophobicity of the poloxamer rather than just the size of the hydrophobic PPO block.

Discussion

To understand the effect of P188 on the structural integrity of the phospholipid membrane, we have systematically examined the leakage dynamics of GUVs under various hypo-osmotic gradients. In the range $0 \leq \Delta\pi \leq 100$ mOsm, GUVs with low membrane tension ($\leq 4.2 \pm 1.9$ mN/m) show two kinds of structural changes: (1) pure swelling and (2) the formation of transient pores, leading to pulse-wise leakage through multiple swelling−bursting cycles. These structural changes are quite similar to what have been observed in living cells subjected to electroshocks,[45] though the osmotic gradients that biological cells experience are much lower than those applied in our current study. The leakage due to the transient pores in the lipid membrane is a consequence of membrane expansion resulting from a lower concentration of osmotically active solutes outside the vesicles. Theoretical calculations show that transient pores appear only after membrane expansion exceeds a threshold value.[33] In our GUVs system, a threshold value of $\sim 1.5 \pm 0.5\%$ in diameter expansion has been observed, in a good agreement with the literature value.[46]

Our P188 short-time incubation results suggest that the resealing effect of P188 in restoring cell membrane integrity may be due to its capability to extend the swelling and subsequently retard the leakage.[33] To achieve the optimal effect, a certain amount of P188 needs to be adsorbed on the membrane surface. Since the dynamics of leakage in our GUVs system is much faster than that of P188 accumulation on the membrane surface, incubating GUVs with P188 for a short period of time produces superior results over perfusion of the polymer over the GUVs. This short-time incubation procedure helps ensure an adequate adsorption of P188 onto the GUV membrane surface prior to the application of an osmotic gradient. This protocol, however, differs from the clinical procedure in which polymers are applied to structurally compromised cells after, as opposed to before, the injury. One possible reason that direct injection of P188 works in live cells is that the biological membrane, which is associated with the cytoskeleton, can expand to a much larger extent, sustain permanent pores, and leak at a much slower rate than free lipid vesicles, thus providing enough time for P188 to adhere to the injured site on the membrane surface.[47]

It is evident that rather than serving as a sealing agent, an extended incubation period with the GUVs turns the triblock copolymer into a permeabilizing agent, as it allows the interaction between P188 and the lipid membrane to go beyond surface adsorption. After a certain period of time, P188 starts to insert into the membrane, which acts to disrupt its structural integrity, as confirmed by our experiments involving preincorporation of P188 and PEG-PE in the membrane. It has been reported that P188 in the clinical setting can only be tolerated by healthy human volunteers for up to 44 h at the most effective dose when the intake is continuous,[48,49] though the origin of the harmful side effect is unknown. On the basis of our data, this transition from the beneficial resealing effect of P188 to its harmful side effect observed in clinical studies can possibly be related to the sealant to permeation enhancer transition observed in our model system from P188 adsorption to P188 insertion into the membrane as a function of incubation time.

Results from our examination of poloxamers with different architecture further suggest that while the adsorption of these poloxamers to the membrane surface is somewhat independent of their architecture, their insertion into membranes is mainly dictated by their hydrophobicity: the more hydrophobic the triblock copolymer, the easier the insertion. While some of the triblock copolymers are ideal candidate for membrane permeation enhancer, like P181, others like the more hydrophilic ones are slow in the insertion and are poor candidates for enhancing permeation. Rather, these hydrophilic copolymers act well as membrane resealing agent. PEG 20 kDa is the extreme case of the latter, which has been shown to be effective in attenuating lung endothelial cell barrier dysfunction[50] and reducing oxidative stress in neurons after injury.[51]

Our results obtained using model GUV systems here bring us one step closer to understanding the intricate interactions between lipids and triblock copolymers and help tease out factors at the molecular level that drive triblock copolymers to act as either membrane resealants or permeation enhancers. The natural mechanism for a cell to restore the integrity of its structurally compromised membrane is a synergetic process involving intracellular lipid vesicles, ions, peptides, proteins, cytoskeletons, etc.[2] For cells sustaining severe structural damage in the membrane, the synergetic membrane healing process could be hampered or simply might not be maintained at a normal level; the administration of exogenous agents like poloxamers, under the correct conditions, can help seal these damaged membranes. Furthermore, there have been reports on the ability of P188 to help proteins refold to their native conformation after thermal denaturation,[52] suggesting that not only could the triblock copolymers directly interact with the lipids in the membrane to retard leakage, but they might also play a key role in the recovery of the synergetic interactions among other biologically relevant components associated with the membrane healing process.

Acknowledgment. This work was supported in part by the National Institutes of Health (1R01 NS056313-01A1 to JM). J.-Y.W. and K.Y.C.L. are grateful for the support of the March of Dimes (No. 6-FY07-357) and the University of Chicago MRSEC program of the NSF (DMR-0820054). J.C. acknowledges the support from the James Franck Institute, the Department of Chemistry, and the College for undergraduate research. We thank Dr. Christine Labno for her help with confocal microscopy imaging and data reconstruction, Marina Bodnarchuk for her help with the ζ-potential measurements, and Wei Chen at UMass-Amherst for his help with Gel Permeation Chromatography (GPC) measurements and acknowledge the University of Chicago MRSEC Shared Facilities and the Integrated Microscopy Core Facility for the usage of their instruments.

(45) Kinosita, K.; Tsong, T. *Nature* **1977**, *268*, 438.
(46) Kwok, R.; Evans, E. *Biophys. J.* **1981**, *35*, 637.
(47) Hoffman, J. F. *J. Gen. Physiol.* **1958**, *42*, 928.
(48) Jewell, R. C.; Knor, S. P.; Kisor, D. F.; LaCrois, K. A.; Wargin, W. A. *J. Pharm. Sci.* **1997**, *86*, 808.
(49) Steinhardt, R. A. *Nature* **2005**, *436*, 925.
(50) Chiang, E. T.; Camp, S. M.; Dudek, S. M.; Brown, M. E.; Usatyuk, P. V.; Zaborina, O.; Alverdy, J. C.; Garcia, J. G. N. *Microvasc. Res.* **2009**, *77*, 174.
(51) Luo, J.; Borgens, R.; Shi, R. *J. Neurotrauma* **2004**, *21*, 994.
(52) Walsh, A. M.; Mustafi, D.; Makinen, M. W.; Lee, R. C. *Ann. N.Y. Acad. Sci.* **2005**, *1066*, 321.

Supporting Information Available: Details in the preparation of GUVs and polymer solutions, the selection of GUVs, and the description of the flow chamber; a series of representative raw data at 40 mOsm gradient to clarify how the statistics were obtained; the analysis on the change in the vesicle volume and comparison to the applied osmolarity difference; the principle and details of ζ-potential measurements and their possible source of errors; the leakage profiles of GUVs upon perfusion of 50 μM P188 at different osmotic gradients; fluorescence images of GUVs indicating the loss of a lipid fragment from the membrane; digital images in comparison of change in the amount of GUVs present (A) in the absence of P188 and (B) with P188 incubation for 1 and 3 days of incubation. This material is available free of charge via the Internet at http://pubs.acs.org.